Bulk and Brane Decay of a (4+n)-Dimensional Schwarzschild-De-Sitter Black Hole: Scalar Radiation

P. Kanti[1], J. Grain[2] and A. Barrau[2]

[1]*Department of Mathematical Sciences, University of Durham, South Road, Durham DH1 3LE, UK*

[2]*Laboratory for Subatomic Physics and Cosmology, Joseph Fourier University, CNRS-IN2P3, 53, avenue de Martyrs, 38026 Grenoble cedex, France*

Abstract

In this paper, we extend the idea that the spectrum of Hawking radiation can reveal valuable information on a number of parameters that characterize a particular black hole background – such as the dimensionality of spacetime and the value of coupling constants – to gain information on another important aspect: the curvature of spacetime. We investigate the emission of Hawking radiation from a D-dimensional Schwarzschild-de-Sitter black hole emitted in the form of scalar fields, and employ both analytical and numerical techniques to calculate greybody factors and differential energy emission rates on the brane and in the bulk. The energy emission rate of the black hole is significantly enhanced in the high-energy regime with the number of spacelike dimensions. On the other hand, in the low-energy part of the spectrum, it is the cosmological constant that leaves a clear footprint, through a characteristic, constant emission rate of ultra-soft quanta determined by the values of black hole and cosmological horizons. Our results are applicable to "small" black holes arising in theories with an arbitrary number and size of extra dimensions, as well as to pure 4-dimensional primordial black holes, embedded in a de Sitter spacetime.

1 Introduction

It has recently been pointed out that the hierarchy problem can be addressed in an elegant geometrical way by assuming the existence of extra dimensions in the Universe [1, 2] (for some early works, see Ref. [3]). If only gravity is allowed to propagate in the $(4+n)$-dimensional bulk while all other fields are confined to a $(3+1)$-dimensional brane, the size of the extra dimensions can be as large as 1 mm and the related fundamental Planck scale, M_*, can be as low as 1 TeV [1]. A distinctive feature of the scenario with Large Extra Dimensions [1] is that, above the scale of decompactification, gravitational interactions become strong, with the highly suppressed 4-dimensional Newton's constant, κ_4^2, being replaced by the significantly larger D-dimensional one, κ_D^2. This idea has driven a considerable interest as it opens exciting possibilities for observing strong gravitational phenomena possibly at the TeV scale.

A particularly exciting proposal is that of the creation of mini black holes [4], either at colliders [5] or in high energy cosmic-ray interactions [6] (for an extensive discussion of the phenomenological implications as well as for a more complete list of references, see the recent reviews [7, 8]). If such black holes do indeed form during high-energy particle collisions, with center-of-mass energies greater than the fundamental Planck scale M_*, we expect them to evaporate through the emission of Hawking radiation, similarly to their 4-dimensional counterparts - for a detailed discussion of the properties of these microscopic black holes formed in a flat, higher-dimensional spacetime, see Refs. [7, 9, 10]. These black holes remain, at least initially, attached to our brane and emit Hawking radiation, in the form of elementary particles, both in the bulk and on the brane. In order to avoid modification of the bulk gravitational background, the self-energy of the brane is assumed to be much smaller than the black hole mass. In addition, the mass of the produced black hole must be, at least, a few times larger than the fundamental Planck scale M_*, so that quantum gravity effects can be safely ignored, as for any classical object.

The emission of Hawking radiation from small black holes with horizon $r_H \ll L$, where L the size of the extra dimensions, formed in a flat, higher-dimensional background, has been the subject of several works during the last couple of years. In the case of a spherically-symmetric Schwarzschild-like black hole, the task of determining the Hawking radiation emission rate has been approached both analytically [11, 12, 13] and numerically [14]. In the first set of works, analytical formulae for the emission rate were derived, but only under certain approximations that limited their validity either at the low- or high-energy regime. The latter numerical analysis [14], though, demonstrated in the most exact way the dependence of the emission rate on the fundamental parameters of the problem, i.e. the energy of the emitted particle, its spin, and, last but not least, the dimensionality of spacetime. In the case of a rotating, Kerr-like black hole in a flat higher-dimensional spacetime, analytical formulae for the emission rate were again derived [15, 16] but the results are only partial, being valid only at the low-energy regime, for low angular momentum of the black hole, and for a specific dimensionality of spacetime.

What these recent works – focused on the emission from a higher-dimensional black hole – have revealed is the extremely important fact that the spectrum of Hawking ra-

diation encodes vital information about the structure of the geometrical background, a feature that was not apparent in the related studies in the 4-dimensional spacetime [17, 18, 19]. Apart from the dimensionality of spacetime, the radiation spectrum may give information on other aspects of the structure of the particular black hole background emitting the radiation. For instance, in Ref. [20], it was demonstrated that, in the case of a higher-dimensional black hole formed in the presence of the higher-derivative, stringy-inspired Gauss-Bonnet term, the radiation spectrum depends also on the value of the coupling constant of the Gauss-Bonnet term.

During past years, significant observational evidence has been obtained favoring a non-zero cosmological constant in the Universe [21]. The presence of a non-trivial vacuum energy in the universe inevitably affects the formation of black holes, and modifies accordingly the gravitational background around them. Since, as we mentioned above, the spectrum of Hawking radiation is highly sensitive to the structure of the particular black hole background, the one emanating from a black hole formed in a curved spacetime will also bear a strong dependence on the value of the cosmological constant. In 4 dimensions, the existing literature consists of only a handful of works that have studied the emission of Hawking radiation coming from a Schwarzschild-de-Sitter (SdS) black hole by either considering two-dimensional toy models [22, 23, 24] or focusing on special cases, like the degenerate case of a SdS spacetime where the black hole and cosmological horizon coincide [25]. Surprisingly enough, in a higher number of dimensions, no work up to now has investigated the exact form of the Hawking radiation spectrum of a SdS black hole, with all the activity having been focused on the study of the pair creation of black holes [26], thermodynamical aspects of radiation via tunneling [27], or the perturbations of the higher-dimensional spacetime [28, 29] and the associated quasinormal frequencies [30] (for related studies in 4 dimensions, see [31]).

This article aims at filling the aforementioned gap in the literature by deriving the exact form of the generalized Hawking radiation spectrum (including the greybody factors) of a Schwarzschild black hole embedded in a D-dimensional de Sitter space-time. In this way, the exact dependence of the radiation spectrum on all the parameters of the theory will be revealed, and the effects of both the dimensionality and the bulk cosmological constant of the higher-dimensional spacetime on the emitted radiation will be determined. From a theoretical point of view, the study of non-asymptotically flat spacetimes is well motivated by the de Sitter (dS) and Anti-de Sitter (AdS) / conformal field theory (CFT) correspondence, and the need to generalize, for a curved background, techniques and principles, developed for a flat spacetime, is obvious. From the observational point of view, the prospect of obtaining information on the topological structure of our spacetime, including its curvature, from the Hawking radiation emitted from small black holes – an effect possibly observable in near or far-future experiments – increases further the importance of this work.

A discussion of the approximations made during our analysis should be added here. In order to avoid any significant back reaction to the gravitational background due to the change in the black hole mass after the emission of a particle, we must assume that $\omega \ll M_{BH}$. Since the emission spectrum is peaked around the black hole temperature, it is

sufficient to assume instead that $T_H \ll M_{BH}$. As we will see in the next section, the temperature of a Schwarszchild-de Sitter black hole is lower than the one of a Schwarzschild black hole, therefore, if the latter satisfies the aforementioned constraint, the former will also do. By using the relation between the horizon and mass for a $(4+n)$-dimensional Schwarzschild black hole, this constraint translates to $M_{BH} \gg M_*$, that is the black hole mass must be much bigger than the fundamental Planck scale. The same bound guarantees that quantum effects are small since such a black hole can be safely considered as a classical object. The frequency of the emitted particles is also bounded from below: in order for these quanta to be considered as $(4+n)$-dimensional, not only the black hole horizon, but also their wavelength must be smaller than the size of the extra dimensions, or equivalently $\omega \gg 1/L$. Throughout our analysis, we will be assuming that the mass of the black hole is indeed much higher than M_*; however, the lower bound on the frequency will be temporarily ignored for the sake of presenting complete emission spectra valid at all energy regimes - this bound will be re-instated and its importance will be discussed in the final discussion of our results at the end of our paper.

The outline of our paper is as follows: in the next section, we describe the general framework for our analysis and briefly discuss the properties of the higher-dimensional SdS black hole. In section 3, we concentrate on the emission of Hawking radiation from a decaying SdS black hole on the brane. We start by considering the line-element describing the-induced-on-the-brane gravitational background, and then we derive the master equation for propagation of fields with arbitrary spin in the 4-dimensional geometry. In this work, we focus on the emission of Hawking radiation in the form of scalar fields, and the corresponding cross-section, or "greybody factor", for emission on the brane is determined, first analytically, in the high- and low-energy limits, and then numerically, in terms of the total number of dimensions and the value of the bulk cosmological constant. The existence of extra dimensions in nature have a strong effect on the emission cross-section, similar to the one found in the case of an asymptotically-flat Schwarzschild black hole; in addition, the presence of the cosmological constant modifies significantly the behaviour of the same quantity both at low and high energies. In section 4, we turn to the emission of Hawking radiation, in the form of scalar fields, in the bulk: we provide again analytical results for the "bulk" greybody factor, in the low- and high-energy regime, and then exact, numerical ones; both sets of results prove the same strong dependence of the cross-section, for emission in the bulk, on the cosmological constant and number of extra dimensions, as on the brane. In Section 5, the final energy emission rates for the "brane" and "bulk" channels are calculated, and the exact Hawking radiation spectra are presented. We comment on the role that the two fundamental background parameters – the cosmological constant and dimensionality of spacetime – play in the formation of the spectra at all energy regimes, and also to the magnitude of the relative emission rate for "bulk" and "brane" emission. The latter quantity is necessary to address the question of the amount of radiation lost in the space transverse to the brane and thus the amount of energy available for emission on the brane. We finish with a summary of our results and conclusions, in section 6.

2   General framework

We start our analysis by presenting the line-element that describes a higher-dimensional, neutral, spherically-symmetric black hole that arises in the presence of a positive cosmological constant. The line-element of the so-called Schwarzschild-de-Sitter (SdS) black hole was first derived in [32], and has the form

$$ds^2 = -h(r)\,dt^2 + \frac{dr^2}{h(r)} + r^2 d\Omega_{2+n}^2, \tag{1}$$

where

$$h(r) = 1 - \frac{\mu}{r^{n+1}} - \frac{2\kappa_D^2\,\Lambda\,r^2}{(n+3)(n+2)}\,. \tag{2}$$

The above line-element describes a black hole living in a D-dimensional spacetime, where n is the number of extra, spacelike dimensions that exist in nature ($D = 4 + n$), and Λ the positive cosmological constant in the bulk. The parameter μ is related to the ADM mass of the black hole through the relation [9]

$$\mu = \frac{2\kappa_D^2 M_{BH}}{(n+2)\,A_{2+n}}\,, \qquad A_{2+n} = \frac{2\pi^{(n+3)/2}}{\Gamma[(n+3)/2]}\,, \tag{3}$$

where A_{2+n} is the area of a unit $(2+n)$-dimensional sphere. In addition, $d\Omega_{2+n}^2$ describes the corresponding line-element of the $(2 + n)$-dimensional unit sphere, and is given by

$$d\Omega_{2+n}^2 = d\theta_{n+1}^2 + \sin^2\theta_{n+1}\left(d\theta_n^2 + \sin^2\theta_n\left(\,...\, + \sin^2\theta_2\left(d\theta_1^2 + \sin^2\theta_1\,d\varphi^2\right)...\right)\right). \tag{4}$$

In the above, $0 < \varphi < 2\pi$ and $0 < \theta_i < \pi$, for $i = 1, ..., n+1$ – notice that due to the assumed spherical symmetry of the problem, n additional azimuthal coordinates θ_i have been introduced to describe the n compact extra dimensions. Finally, in Eq. (2), the parameter $\kappa_D^2 = 1/M_*^{2+n}$ stands for the $(4 + n)$-dimensional Newton's constant.

Due to the presence of the positive cosmological constant Λ in the bulk, the higher-dimensional spacetime is not asymptotically-flat. The spacetime has a true curvature singularity at $r = 0$, and the equation

$$h(r_i) = 1 - \frac{\mu}{r_i^{n+1}} - \frac{2\kappa_D^2\,\Lambda\,r_i^2}{(n+3)(n+2)} = 0\,, \tag{5}$$

will yield, in principle, $(n + 3)$ roots r_i which correspond to $(n + 3)$ horizons for this spacetime. However, due to the positivity of r, only two real, positive roots emerge, the largest one (r_C) corresponding to the Cosmological horizon, and the smallest one (r_H) to the Black Hole event horizon. The metric function $h(r)$ is therefore interpolating between two zeros, one at $r = r_H$ and one at $r = r_C$. The behaviour in between is easily found by looking at the first derivative, $h'(r)$: this function becomes zero only at the point

$$r_0 = \left[\frac{(n+1)(n+2)(n+3)\mu}{4\kappa_D^2\Lambda}\right]^{1/(n+3)}, \tag{6}$$

4

that is easily found to correspond to a global maximum. Therefore, $h(r)$ increases for $r > r_H$, reaches a maximum at $r = r_0$, and decreases again towards zero for $r_0 < r < r_C$.

The temperature of the black hole is given in terms of the surface gravity at the location of the horizon [1], i.e.

$$T_H = \frac{k_H}{2\pi} = \frac{1}{4\pi r_H} \left[(n+1) - \frac{2\kappa_D^2 \Lambda}{(n+2)} r_H^2 \right]. \tag{7}$$

In the above, we have used the relation that follows from Eq. (5), i.e.

$$\mu = r_i^{n+1} \left[1 - \frac{2\kappa_D^2 \Lambda}{(n+2)(n+3)} r_i^2 \right], \tag{8}$$

evaluated at $r_i = r_H$, to eliminate the parameter μ from the expression for the temperature of the black hole. The temperature of the universe is given by a similar expression in terms of the surface gravity of the cosmological horizon

$$T_C = \frac{k_C}{2\pi} = -\frac{1}{4\pi r_C} \left[(n+1) - \frac{2\kappa_D^2 \Lambda}{(n+2)} r_C^2 \right], \tag{9}$$

where care has been taken to ensure that T_C is positive. Since $r_C > r_H$, the temperature of the universe will always be smaller than that of the black hole, $T_C < T_H$.

As any black hole with a non-vanishing temperature, the Schwarzschild-de-Sitter black hole will emit Hawking radiation [33] in the form of elementary particles. The emission will take place in the higher-dimensional spacetime (1) with the corresponding flux spectrum, i.e. the number of particles emitted per unit time, given by

$$\frac{dN^{(s)}(\omega)}{dt} = \sum_j \sigma_{j,n}^{(s)}(\omega) \frac{1}{\exp(\omega/T_H) \pm 1} \frac{d^{n+3}k}{(2\pi)^{n+3}}. \tag{10}$$

The above formula is a direct generalization of the corresponding four-dimensional expression [33] for a higher number of dimensions. In the above, s is the spin of the emitted degree of freedom and j its angular momentum quantum number. The spin statistics factor in the denominator is -1 for bosons and $+1$ for fermions. The corresponding power spectrum, i.e. the energy emitted per unit time by the black hole, can be easily found by combining the number of particles emitted with the amount of energy they carry. It is given by

$$\frac{dE^{(s)}(\omega)}{dt} = \sum_j \sigma_{j,n}^{(s)}(\omega) \frac{\omega}{\exp(\omega/T_H) \pm 1} \frac{d^{n+3}k}{(2\pi)^{n+3}}. \tag{11}$$

For massless particles, $|k| = \omega$ and the phase-space integral reduces to an integral over the energy of the emitted particle ω. In what follows we are going to focus on the emission of massless particles, or on particles with a rest mass much smaller than the temperature

---

[1]In section 5, a more accurate definition of the temperature of a black hole embedded in a de Sitter spacetime will be given - for the purpose of our analysis up to section 5, the above definition is sufficient.

of the black hole. Note that, since $T_H > T_C$, there will always be a net flow of energy from the black hole towards the universe.

Both expressions, Eqs. (10) and (11), contain an additional factor, $\sigma_{j,n}^{(s)}(\omega)$, which stands for the cross-section for the emission of a particle from a black hole, or alternatively, the "greybody factor". In a blackbody radiation spectrum, this factor is constant, and equal to the area of the emitting body. In the case of a black hole, however, it depends on the energy of the emitted particle, its spin and its angular momentum number, and therefore, we expect it to significantly modify the Hawking radiation spectrum. The greybody factor can be computed by determining the absorption probability, $|\mathcal{A}_{j,n}^{(s)}|^2$, for propagation in the aforementioned higher-dimensional background (1), and then using the generalised $(4+n)$-dimensional optical theorem relation [34]

$$\sigma_{j,n}^{(s)}(\omega) = \frac{2^n \pi^{(n+1)/2}\, \Gamma[(n+1)/2]}{n!\, \omega^{n+2}}\, \frac{(2j+n+1)\,(j+n)!}{j!}\, |\mathcal{A}_{j,n}^{(s)}|^2\,. \qquad (12)$$

We should finally stress here the extremely important fact that the greybody factor depends also on the dimensionality of spacetime, and as we will see, in the case of a non-asymptotically flat spacetime, on the value of the bulk cosmological constant, too. Therefore, the corresponding black hole radiation spectrum encodes valuable information for the structure of the spacetime around the black hole, including the number of dimensions and the curvature of the spacetime in which the black hole lives. It is this double-fold dependence of the black hole radiation spectrum that we are planning to investigate in this work.

3   Hawking radiation from a $(4+n)$-Dimensional SdS Black Hole on the Brane

In this section, we will concentrate on the emission of Hawking radiation on the brane from a decaying higher-dimensional Schwarzschild-de-Sitter black hole. We will first present the line-element describing the geometry of the induced on the brane gravitational background, and then write the general equation for the propagation of a field with arbitrary spin s in this geometry. By solving this equation both analytically (under certain approximations) and numerically, the greybody factor for scalar emission on the brane from the black hole will be determined.

3.1   General equation for spin-s particles on the brane

Having described the higher-dimensional spacetime in Section 2, we now turn our attention to the induced geometry on the 4-dimensional brane. This simply follows by fixing the values of the 'extra' angular azimuthal coordinates, i.e. $\theta_i = \pi/2$, for $i = 2, ..., n+1$. This leads to the projection of the higher-dimensional line-element (1) on a 4-dimensional slice

that plays the role of our 4-dimensional world. The projected line-element has the form

$$ds^2 = -h(r)\, dt^2 + \frac{dr^2}{h(r)} + r^2 \left(d\theta^2 + \sin^2\theta\, d\varphi^2 \right), \tag{13}$$

where the subscript '1' from the remaining azimuthal coordinate has been dropped. Note that the metric function $h(r)$ remains unchanged during the projection and is still given by Eq. (2), therefore, its profile along the r-coordinate – that now has components only along the 3 non-compact spatial dimensions – remains the same.

All particles restricted to live on the 4-dimensional brane propagate in the projected background (13). The equations of motion, for particles with arbitrary spin s, in a curved background can be derived by using the Newman-Penrose formalism [35, 36]. Under the assumption of minimal coupling with gravity, and by employing the factorized ansatz

$$\Psi_s(t, r, \theta, \varphi) = e^{-i\omega t}\, e^{im\varphi}\, \Delta^{-s}\, P_s(r)\, S^m_{s,j}(\theta), \tag{14}$$

the free equations of motion for particles with spin $s = 0, \frac{1}{2}$ and 1 may be combined to form a 'master' equation, satisfied by the radial part of the field, $P_s(r)$. A master equation for propagation in the projected on the brane background of a $(4+n)$-dimensional rotating black hole was derived in [7] (see also [16]). In the limit of zero black hole angular momentum, the line-element used in [7] reduces exactly to the spherically-symmetric one given in Eq. (13). In that case, the master equation takes the form

$$\Delta^s \frac{d}{dr} \left(\Delta^{1-s} \frac{dP_s}{dr} \right) + \left(\frac{\omega^2 r^2}{h} + 2is\,\omega\, r - \frac{is\omega\, r^2 h'}{h} - \tilde{\lambda} \right) P_s = 0, \tag{15}$$

where $\Delta \equiv hr^2$, and $\tilde{\lambda} = \lambda + 2s$. The eigenvalue λ is defined through the angular 'master' equation, satisfied by $S^m_{s,j}(\theta)$ – the so-called spin-weighted spherical harmonics [37]; this has the form [7]

$$\frac{1}{\sin\theta} \frac{d}{d\theta} \left(\sin\theta \frac{dS^m_{s,j}}{d\theta} \right) + \left[-\frac{2ms\cot\theta}{\sin\theta} - \frac{m^2}{\sin^2\theta} + s - s^2\cot^2\theta + \lambda \right] S^m_{s,j} = 0. \tag{16}$$

It was found that $\lambda \equiv j\,(j+1) - s\,(s+1)$, and thus $\tilde{\lambda} = j\,(j+1) - s\,(s-1)$. We should note here that ω is the energy of the propagating particle, s its spin and j its angular momentum quantum number.

Equation (15) was used in Refs. [11, 13, 14] to study the emission of scalars, fermions, and gauge bosons by a $(4+n)$-dimensional Schwarzschild black hole on the brane. In the presence of a cosmological constant in the bulk, the exact expression of the metric function $h(r)$ changes and assumes the form (2), but both projected line-elements have the same general structure given in Eq. (13). Therefore, Eq. (15) can also be used to study propagation of fields with arbitrary spin s in the projected background of a higher-dimensional Schwarzschild-de-Sitter black hole, and thus the emission of Hawking radiation from such a black hole on the brane. This task, for the emission of scalar fields, will be performed in the next two subsections: we will first derive analytically the low- and high-energy limit of the greybody factor, and then we will proceed to derive exact numerical results for the same quantity.

3.2 Analytical results for scalar emission on the brane

To determine the greybody factor $\sigma_{j,n}^{(s)}(\omega)$, one needs to find first the absorption coefficient $\mathcal{A}_{j,n}^{(s)}(\omega)$ for propagation of a field in the projected background (13). To this end, we need to solve the radial equation (15) over the whole radial regime. Even in the absence of a bulk cosmological constant, the general solution of this equation is extremely difficult to be found. In Refs. [11, 13], where the emission of Hawking radiation from a higher-dimensional Schwarzschild black hole was studied, this equation was solved analytically at the low-energy regime, i.e. for $\omega r_H \ll 1$, by making use of a well-known approximation method: the solutions in the near-horizon and far-field regimes were found and then smoothly matched in the intermediate zone. This led to an analytical expression for the absorption coefficient as a function of the energy ω, the spin s, the total angular momentum number j, and the number of extra dimensions n [11, 13].

In the presence of a cosmological constant in the bulk though, even the use of this approximate method becomes extremely complicated, and the derivation of a general analytical formula for the absorption coefficient is highly non-trivial. Nevertheless, by using an alternative method, a less general but still analytical expression for the absorption coefficient at the low-energy regime can be derived. The method amounts to solving the radial equation in an intermediate zone, away from the two horizons r_H and r_C, in the infrared limit of $\omega \rightarrow 0$. This solution is then stretched towards the two horizons, and matched with the two asymptotic solutions there. An analytical formula for the absorption coefficient can be easily derived by looking at the $\ell = 0$ partial wave, that, as we will see, gives the dominant contribution to the absorption coefficient. This method was used successfully in 4 dimensions ($n = 0$) to derive a simplified analytical expression for the absorption coefficient in the case of a Reissner-Nordstrom [38] and Schwarzschild-de-Sitter [39] spacetime.

To our knowledge, a similar analysis for the case of a higher-dimensional SdS spacetime projected onto a 4-dimensional brane has never been performed up to now. In what follows we will address this question and concentrate on the case of scalar fields – we will thus drop the spin index $s = 0$ from the various quantities and replace j by ℓ, the orbital angular momentum quantum number. Then, the radial equation (15) will take the simpler form

$$\frac{d}{dr}\left(h\,r^2\,\frac{dP}{dr}\right) + \left[\frac{\omega^2 r^2}{h} - \ell(\ell+1)\right]P = 0\,. \tag{17}$$

In the intermediate zone away from the two horizons, and in the infrared limit of $\omega \rightarrow 0$, the first term inside the square brackets can be ignored. The remaining equation can then be integrated to derive the low-energy solution for $P(r)$, for arbitrary ℓ. In order to simplify our calculations, we will concentrate directly on the mode $\ell = 0$. Then, by using the definition of $h(r)$, Eq. (2), the solution of the above equation, for an arbitrary number of transverse dimensions n, takes the form

$$P(r) = C_1 \left[\frac{\log(r - r_H)}{2k_H r_H^2} - \frac{\log(r_C - r)}{2k_C r_C^2} + \sum_{m=1}^{n+1} \frac{\log(r + r_m)}{2k_m r_m^2}\right] + C_2\,. \tag{18}$$

8

In the above expression, C_1 and C_2 are integration constants to be determined shortly, and the r_m's stand for the $n+1$ negative roots of the equation $h(r) = 0$. Finally, the quantity

$$k_i = \frac{1}{2} \frac{dh}{dr}\bigg|_{r=r_i} = \frac{1}{2r_i}\left[(n+1) - \frac{2\kappa_D^2 \Lambda}{n+2} r_i^2\right], \tag{19}$$

is the surface gravity at the location of the ith root, including r_H and r_C. As it is clear from Eq. (18), in the limits $r \to r_H$ and $r \to r_C$, the first and second term, respectively, will be the dominant one in each case with the remaining ones acquiring a constant value.

The solution near the two horizons can be alternatively found by solving the radial equation (17) directly in the limits $r \to r_H$ and $r \to r_C$, a task that is greatly facilitated if we make use of the so-called 'tortoise' coordinate, defined by the relation

$$\frac{dr_*}{dr} = \frac{1}{h(r)}. \tag{20}$$

Defining also a new radial function through the relation $u(r) = rP(r)$, Eq. (17) takes the Schrödinger-like form

$$-\frac{d^2 u}{dr_*^2} + h(r)\left[\frac{\ell(\ell+1)}{r^2} + \frac{h'(r)}{r}\right] u = \omega^2 u, \tag{21}$$

or, more explicitly,

$$-\frac{d^2 u}{dr_*^2} + h(r)\left[\frac{\ell(\ell+1)}{r^2} + \frac{\mu(n+1)}{r^{n+3}} - \frac{4\kappa_D^2 \Lambda}{(n+2)(n+3)}\right] u = \omega^2 u. \tag{22}$$

From the above equation, we may easily read the gravitational potential barrier $V(r)$ that a scalar particle sees while propagating from the cosmological to the black hole horizon or vice versa. As an illuminating example, Fig. 1 depicts the form of this barrier for $n = 1$, $\mu = 1$, $\Lambda r_H^2 = 10^{-2}$ (henceforth, the values of the latter two quantities will be given in terms of Planck units, i.e. M_*^{n+1} and M_*^{2+n}, respectively) and $\ell = 0, 1$ and 2. We notice that the barrier takes its lowest possible value for the partial wave $\ell = 0$, therefore, it is this mode that is more likely to be emitted by the black hole, with the emission of higher partial waves being considerably suppressed – our decision, therefore, to consider only the lowest partial wave in our analytical approach is justified. Since the metric function $h(r)$ vanishes at both horizons, r_H and r_C, so does the potential barrier that is proportional to the metric function. Therefore, in both of these regimes, the solution for u will have the form of plane waves. We may therefore write

$$u(r_*) \simeq A_1 e^{-i\omega r_*}, \quad \text{for} \quad r \simeq r_H, \tag{23}$$

$$u(r_*) \simeq B_1 e^{-i\omega r_*} + B_2 e^{i\omega r_*}, \quad \text{for} \quad r \simeq r_C. \tag{24}$$

The solution near the black hole horizon, Eq. (23) has been written in such a way as to satisfy the boundary condition that only incoming modes must exist in this area – no such condition exists for the solution at the cosmological horizon, which therefore includes both incoming and outgoing modes.
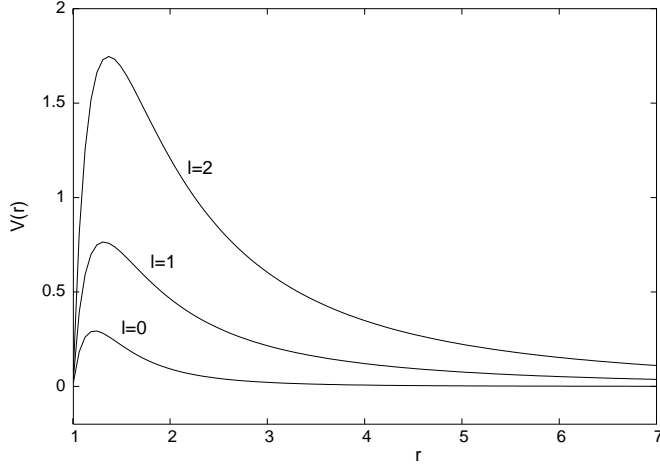
9

Figure 1: *The gravitational potential barrier $V(r)$ in the projected 4-dimensional SdS spacetime for $n = 1$, $\mu = 1$, $\Lambda r_H^2 = 10^{-2}$ and $\ell = 0, 1$ and 2. The barrier vanishes at $r_H = 1.0008$ and $r_C = 24.474$.*

By using the definition (2), Eq. (20) can be integrated to give

$$r_* = \frac{\log(r - r_H)}{2k_H} - \frac{\log(r_C - r)}{2k_C} + \sum_{m=1}^{n+1} \frac{\log(r + r_m)}{2k_m}. \tag{25}$$

In the low-energy limit, the asymptotic solution near the black hole horizon $(r \to r_H)$, Eq. (23), can be written as

$$u^{(B)}(r) \simeq A_1 \left\{ 1 - i\omega \left[\frac{\log(r - r_H)}{2k_H} - \frac{\log(r_C - r_H)}{2k_C} + \sum_{m=1}^{n+1} \frac{\log(r_H + r_m)}{2k_m} \right] \right\}. \tag{26}$$

Comparing the above with the function $rP(r)$, taken in the limit $r \to r_H$, we find that

$$C_1 = -i\omega r_H A_1, \qquad C_2 = \frac{A_1}{r_H} + \mathcal{O}(\omega). \tag{27}$$

A similar low-energy expansion of the asymptotic solution (24), near the cosmological horizon r_C, yields the following expression

$$u^{(C)}(r) \simeq (B_1 + B_2) + i\omega \left(-B_1 + B_2 \right) \left[\frac{\log(r_C - r_H)}{2k_H} - \frac{\log(r_C - r)}{2k_C} + \sum_{m=1}^{n+1} \frac{\log(r_C + r_m)}{2k_m} \right] \right\}. \tag{28}$$

Comparing again the expressions of $rP(r)$, in the limit $r \to r_C$, and $u^{(C)}(r)$, we are led to the relations

$$C_1 = i\omega r_C \left(-B_1 + B_2 \right), \qquad C_2 = \frac{1}{r_C} \left(B_1 + B_2 \right) + \mathcal{O}(\omega). \tag{29}$$

As it is clear from the asymptotic solutions (23)-(24), the reflection coefficient for the propagation of a scalar field in this background will be given by the ratio B_2/B_1, that

10

can easily follow by combining Eqs. (27) and (29). Then, the corresponding reflection and absorption probabilities are found to be

$$|\mathcal{R}_{0,n}|^2 = \left|\frac{B_2}{B_1}\right|^2 = \frac{(r_C^2 - r_H^2)^2}{(r_C^2 + r_H^2)^2}\,, \qquad |\mathcal{A}_{0,n}|^2 = 1 - |\mathcal{R}_{0,n}|^2 = \frac{4r_C^2 r_H^2}{(r_C^2 + r_H^2)^2}\,. \qquad (30)$$

The above results must be contrasted with the ones that follow in the case of propagation of a scalar field in the projected background of a Schwarzschild-like higher-dimensional black hole. A detailed analytical calculation in Ref. [11] showed that, in the absence of a bulk cosmological constant, the absorption coefficient is given by: $\mathcal{A}_{\ell,n} \propto (\omega r_H)^{\ell+1}$, and therefore vanishes in the low-energy limit for all values of ℓ. On the other hand, similar results to the ones shown in Eqs. (30) were derived also in the case of a scalar field being scattered in the interior of a Reissner-Nordstrom black hole (i.e. between the Cauchy and the event horizon) [38], and in the area between the black hole and cosmological horizon of a 4-dimensional Schwarzschild-de-Sitter black hole [39]. The deciding factor therefore, for the value of the absorption coefficient in the infrared limit, is the presence or not of a second horizon that creates a finite-size universe in which the particle propagates – a particle with zero energy, i.e. infinite wavelength, cannot be localized, and thus has a finite probability to traverse the finite distance between the two horizons. As it was shown in Ref. [39], constant field configurations, that have a vanishing energy-momentum tensor and thus zero energy, do exist in a SdS background, therefore, we expect an enhancement in the emission of ultra-soft quanta compared to the case of an asymptotically-flat spacetime. We notice that, in the limit $\Lambda \to 0$, or $r_C \to \infty$, the absorption coefficient vanishes, as expected for the scattering of a zero-energy scalar particle in a single-horizon area.

Although the functional dependence of the absorption probability on the two horizons, r_H and r_C, is the same as in the case of a pure 4-dimensional SdS spacetime, our result has an implicit dependence on the value n of the transverse spacelike dimensions as well as on the value of the bulk cosmological constant. The dependence on both of these parameters is depicted on the entries of Table 1, for $\mu = 1$. For fixed Λ, the absorption probability reduces as the number of extra dimensions increases, a behaviour that was also encountered in the case of propagation of a scalar field in a projected Schwarzschild-like black hole background on the brane. On the other hand, for fixed n, the presence of an increasingly larger bulk cosmological constant enhances the value of the absorption probability at the low-energy regime, and thus facilitates the emission of scalar fields from the black hole on the brane. The dependence of the absorption probability on n and Λ could have also been inferred from the qualitative dependence of the effective potential $V(r)$ on these two parameters: keeping ℓ fixed, the height of the barrier increases as n increases, while it decreases as Λ increases.

Table 1: Absorption probabilities for emission on the brane in the limit $\omega \to 0$

n	$|\mathcal{A}_{0,n}|^2$ (for $\Lambda r_H^2 = 10^{-2}$)	$\mathbf{\Lambda r_H^2}$	$|\mathcal{A}_{0,n}|^2$ (for $n = 1$)
0	0.01417	0	0
1	0.00667	10^{-4}	6.67×10^{-5}
2	0.00340	10^{-3}	6.76×10^{-4}
3	0.00266	10^{-2}	6.67×10^{-3}
5	0.00142	$10^{-1.5}$	2.11×10^{-2}
7	0.00088	10^{-1}	6.67×10^{-2}

Let us now turn to the high-energy regime, where the greybody factor assumes its geometrical optics limit value. This limiting value has been successfully used in 4-dimensional black hole backgrounds to describe the greybody factor of the corresponding black hole [18, 19, 40]. This technique makes use of the geometry around the emitting (or absorbing) body and can be clearly used to perform the same calculation in more complicated gravitational backgrounds. In particular, the same principle was used to derive the greybody factor, in the high-energy regime, of a higher-dimensional Schwarzschild black hole projected onto the brane [41, 14]. We will apply here the same method for a SdS projected black hole: for a massless particle in a circular orbit around a black hole, described by the line-element (13), we write its equation of motion, $p^\mu p_\mu = 0$, in the form

$$\left(\frac{1}{r} \frac{dr}{d\varphi} \right)^2 = \frac{1}{b^2} - \frac{h(r)}{r^2} \,, \tag{31}$$

where b is the ratio of the angular momentum of the particle over its linear momentum. Clearly, the classically accessible regime is defined by the relation $b < \min(r/\sqrt{h})$. The structure of the particular gravitational background enters in the above relation through the metric function $h(r)$. Using the definition (2) and minimising the function $r/\sqrt{h}$, we find that the maximum value of b, i.e. the closest the particle can get to the black hole before getting absorbed, is given by

$$b_c = r_H \left\{ \left(\frac{n+1}{n+3} \right) \left(\frac{n+3}{2} \left[1 - \frac{2\kappa_D^2 \Lambda r_H^2}{(n+2)(n+3)} \right] \right)^{-2/(n+1)} - \frac{2\kappa_D^2 \Lambda r_H^2}{(n+2)(n+3)} \right\}^{-1/2} . \tag{32}$$

Then, the corresponding area, $\sigma_g = \pi b_c^2$, defines the absorptive area of the black hole at high energies and, thus, its greybody factor – being a constant, the emitting body is characterized at high energies by a blackbody radiation spectrum. For $n = 0$ and $\Lambda = 0$, the above expression reduces to the four-dimensional one, $\sigma_g = 27\pi r_H^2/4$ [19, 40]. For $\Lambda = 0$ but $n \neq 0$, we recover the expression for the greybody factor at high energies of a $(4+n)$-dimensional Schwarzschild black hole projected onto a brane [41, 14]. The general expression (32) has a strong dependence on the values of both the bulk cosmological constant and the number of extra dimensions. If we keep Λ fixed and vary n, we obtain a suppression of σ_g as n increases, similar to the one found in the case of brane emission

of scalar fields from a projected Schwarzschild black hole [41, 14]. On the other hand, if we fix n and vary Λ, the greybody factor is enhanced as Λ increases. Therefore, at the high-energy regime, the presence of a bulk cosmological constant and a number of transverse-to-the-brane dimensions have an increasing and decreasing, respectively, effect on the emission cross-section of scalar fields from a projected SdS black hole. The entries of Table 2 show the dependence of the greybody factor at high-energies for some indicative values of n and Λ, and for $\mu = 1$.

Table 2: Greybody factors for emission on the brane in the high-energy limit

n	(for $\Lambda r_H^2 = 10^{-2}$) σ_g (πr_H^2)	Λr_H^2	(for $n = 0$) σ_g (πr_H^2)	(for $n = 1$) σ_g (πr_H^2)
0	6.8591	0	6.7500	4.0000
1	4.0201	10^{-4}	6.7511	4.0002
2	3.0774	10^{-3}	6.7607	4.0020
3	2.6017	10^{-2}	6.8591	4.0201
5	2.1179	$10^{-1.5}$	7.1114	4.0645
7	1.8699	10^{-1}	8.0962	4.2131

3.3 Numerical results for the greybody factor on the brane

To accurately evaluate the greybody factor in a wide energy range, and not only in the low and high-energy regimes, it is necessary to go through numerical computations. For this purpose, we first need to solve the scalar equation (17) for propagation on the brane, and then to extract the amplitudes of the *incoming* and *outgoing* waves at the two asymptotic regimes close to the two horizons. The integration starts at the horizon of the black hole, where the 'no-outgoing' wave boundary condition can be easily applied, and is propagated until the cosmological event horizon. Finally, the amplitudes of the *incoming* and *outgoing* waves are extracted by fitting the analytical asymptotic solutions to the numerical results, and the absorption cross-section (or, greybody factor) $\sigma_{\ell,n}(\omega)$ is then calculated in terms of the absorption probability $|\mathcal{A}_{\ell,n}|^2$.

A number of approximations have to be made in our numerical computation. First, in order to get rid of the apparent singularity at $r = r_H$, the boundary condition at the black hole horizon is applied at $r = r_H + \varepsilon$, where ε must be checked to be small enough so that our results are stable. Furthermore, for each energy point, the sum over the angular momenta ℓ, which defines the greybody factor $\sigma_n(\omega)$, must be truncated at rank m, where m has to be determined so that the error to the value of the absorption cross section from omitting the modes with $\ell > m$ is smaller than the accuracy of our calculation and thus irrelevant.

For the needs of the numerical integration of Eq. (17), the vanishing *outgoing* wave boundary condition (23), applied at $r = r_H + \varepsilon$, can be alternatively written as:

$$P(r) = 1 \tag{33}$$

$$\frac{dP}{dr} = -\frac{i\omega}{h(r)}. \tag{34}$$

Such a choice not only ensures a vanishing *outgoing* wave at the black hole horizon but also an incoming flux, in the same regime, equal to $|P|^2 = 1$ – as our analytical arguments showed, the value of the integration constant A_1 at the black hole horizon does not have an observable effect, and therefore it can be safely set, for simplicity, equal to unity.

Starting from the above asymptotic solution at the black hole horizon, the numerical integration is then propagated towards the cosmological horizon. As the latter horizon is approached, the consistency of the numerical computation requires to vary the integration step according to the blue-shift suffered by the wave function. According to the analytical arguments of the previous subsection, in this asymptotic spacetime region, the radial wave function is the superposition of *incoming* and *outgoing* plane waves:

$$P(r) = B_1 \, e^{-i\omega r_*} + B_2 \, e^{i\omega r_*}, \tag{35}$$

where the tortoise coordinate r_* is given by Eq. (20). The above asymptotic solution is particularly convenient for small values of the bulk cosmological constant, when $r_C \gg r_H$ and the two asymptotic regimes of the black hole and cosmological horizon are far apart. For larger values of Λ though, an alternative far-field asymptotic solution can be used instead: by making the change of variable

$$r \rightarrow f(r) = h(r) \left[1 - \frac{2\kappa_D^2 \Lambda r^2}{(n+2)(n+3)} \right]^{-1}, \tag{36}$$

and the field redefinition $P(f) = f^\alpha \, (1-f)^\beta \, F(f)$, the scalar equation (17) takes, near the cosmological horizon, the form of a hypergeometric equation[2], that finally leads to the solution

$$\begin{aligned}
P(f) = B_1 \, f^\alpha \, (1-f)^\beta \, F(a,b,c;f) \\
+ B_2 \, f^{-\alpha} \, (1-f)^\beta \, F(a-c+1,b-c+1,2-c;f).
\end{aligned} \tag{37}$$

In the above, the indices (a,b,c) and power coefficients (α,β) depend on the fundamental parameters of the problem, i.e. the energy ω of the particle, the angular momentum number ℓ, the number of extra dimensions n, the value of the cosmological constant Λ, and the cosmological horizon r_C. In the limit $r \rightarrow r_C$, the aforementioned solution takes the asymptotic form

$$P(r) = B_1 \, e^{-i\frac{\omega \, r_C}{A_C} \log[f(r)]} + B_2 \, e^{i\frac{\omega \, r_C}{A_C} \log[f(r)]}, \tag{38}$$

---

[2]The analysis leading to the derivation of the hypergeometric equation and to the asymptotic solution near the cosmological horizon is similar to the one followed in Refs. [11, 13, 7].
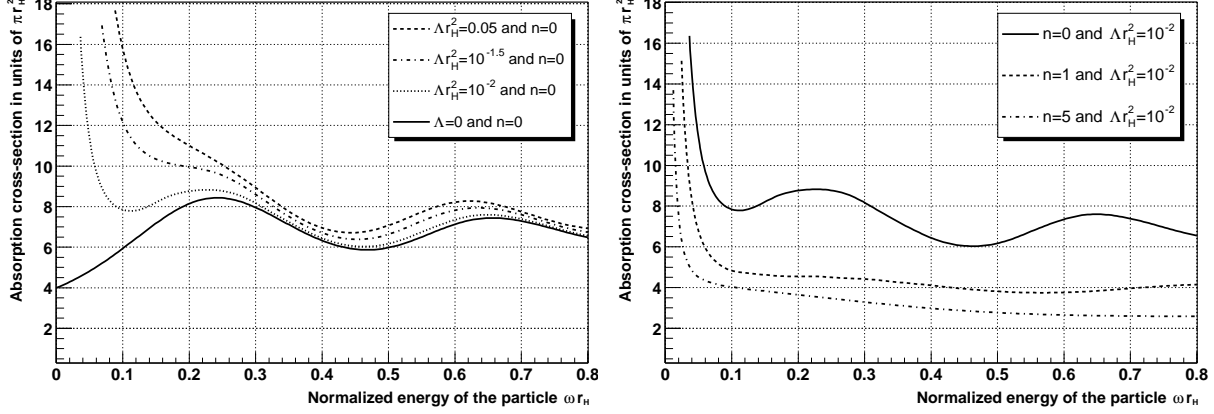
Figure 2: *The absorption cross-section $\sigma_n(\omega)$, for scalar emission on the brane, versus the dimensionless parameter ωr_H: (a) in the first graph, the dimensionality of spacetime is fixed at $n = 0$, while Λr_H^2 takes the values $\{0, 10^{-2}, 10^{-1.5}, 0.05\}$; (b) in the second graph, the cosmological constant is fixed at $\Lambda r_H^2 = 10^{-2}$, while n takes the indicative values $\{0, 1, 5\}$.*

where $A_C = (n+1) - \frac{2\kappa_D^2 \Lambda}{(n+2)} r_C^2$. The above asymptotic solution takes better into account the curvature of the spacetime due to the presence of the bulk cosmological constant, and provides a better fit to our numerical results. Furthermore, the extraction of the *incoming* and *outgoing* amplitudes is straightforward. The new variable $f(r)$ has a profile along the radial coordinate similar to the one of $h(r)$: it vanishes at $r = r_H$ and $r = r_C$ while it reaches a maximum value at some point in between. Near the cosmological horizon, therefore, $\log[f(r)]$ decreases as r increases; taking also into account that A_C is always negative, we may easily conclude that B_1 is the amplitude of the *incoming* wave and B_2 the amplitude of the *outgoing* wave with respect to the black hole horizon.

The absorption cross-section for the emission of fields on the brane follows from the general expression (12) by setting $n = 0$. In addition, the absorption probability $|\mathcal{A}_{\ell,n}|^2$ can be directly determined from the ratio of the incoming fluxes at the cosmological and black hole horizon [7]. We can then write the simple relation:

$$\sigma_{\ell,n}(\omega) = \frac{2\ell + 1}{\omega^2} |\mathcal{A}_{\ell,n}|^2 = \frac{2\ell + 1}{\omega^2} \left| \frac{1}{B_1} \right|^2. \tag{39}$$

Figures 2(a,b) show the results obtained for $\sigma_n(\omega)$ for scalar particles, after the summation over ℓ has been performed, and its dependence on the value of the cosmological constant Λ and the number of extra dimensions n, respectively. In Fig. 2a, the number of extra dimensions has been kept fixed, at $n = 0$, while the value of Λ is allowed to vary. These numerical results are in good agreement with the analytical ones, derived in the previous subsection, both in the low and high-energy regime. When a positive cosmological constant is introduced, the presence of the second (cosmological) horizon causes the absorption probability $|\mathcal{A}_n|^2$ to acquire a non-vanishing value at low energies, which then causes a

15

divergence in the value of $\sigma_n(\omega)$, as $\omega \to 0$, due to the ω^{-2} coefficient in Eq. (39). As a result, the well-known relation at the low-energy limit between the greybody factor and the area of the horizon [19, 11, 14, 43] ceases to hold in the presence of a non-vanishing Λ. In accordance to the entries of Tables 1 and 2, an increase in the value of the cosmological constant causes an enhancement in the value of the greybody factor, with the effect being more significant in the low-energy regime. In the high-energy regime, the effect of the cosmological constant is less significant, nevertheless, as it can be seen from the above curves, the geometrical optics limit of the absorption cross-section does slightly increase as a function of Λ, in agreement with the analytical results of the previous subsection.

The existence of additional dimensions in the universe also modifies the behaviour of the absorption cross-section, as shown in Fig. 2b. In the low energy regime, an increase in the number of extra dimensions n, for a given value of Λ, leads to a suppression of the value of the absorption cross-section. This can be easily understood by noticing that increasing the number of dimensions n leads to an increase in the value of the cosmological horizon r_C, which is equivalent to decreasing the value of Λ. In the high-energy limit, the effect of the dimensionality of spacetime is the same as for asymptotically-flat spacetimes [14] : $\sigma_n(\omega)$ is suppressed as n increases. The behaviour obtained for the greybody factor as a function of n, both in the low and high-energy regime, are in excellent agreement with the analytical results and the entries of Tables 1 and 2 presented in section 3.2.

4 Hawking radiation from a $(4 + n)$-Dimensional SdS Black Hole in the Bulk

According to the assumptions of the model, Standard Model fields (fermions, gauge bosons, Higgs fields) are restricted to live on the 4-dimensional brane, and therefore have no access to the transverse dimensions. Nevertheless, scalar particles that carry no charges under the Standard Model gauge group are in principle allowed to propagate in the bulk. Thus, in the study of the process of the emission of Hawking radiation from a higher-dimensional black hole into the bulk, scalar fields, apart from gravitons, should also be considered. Although this part of radiation would clearly be invisible to an observer on the brane, estimating the amount of energy lost in the "bulk" channel is imperative before accurate predictions for the emitted radiation on the brane can be made.

The field equation describing the motion of a scalar particle in a higher-dimensional background is easy to find. For a free scalar field minimally coupled to gravity, its equation of motion takes the form $D_M D^M \phi = 0$, where D_M is the covariant derivative in the higher-dimensional spacetime. For a spherically-symmetric, $(4 + n)$-dimensional gravitational background of the form (1), this equation takes a separable form if we use the factorized ansatz

$$\phi(t, r, \theta_i, \varphi) = e^{-i\omega t} P(r) \tilde{Y}_\ell(\Omega) , \tag{40}$$

where $\tilde{Y}_\ell(\Omega)$ is the $(3 + n)$-spatial-dimensional generalisation of the usual spherical harmonic functions depending on the angular coordinates [42]. Upon using this ansatz, the

scalar wave equation reduces to a second-order differential equation for the radial wave-function $P(r)$:

$$\frac{h(r)}{r^{n+2}} \frac{d}{dr}\left[h(r)\,r^{n+2}\,\frac{dP}{dr}\right] + \left[\omega^2 - \frac{h(r)}{r^2}\,\ell\,(\ell+n+1)\right]P = 0\,. \qquad (41)$$

The explicit dependence of the above equation on the dimensionality of spacetime is evident: it comes from the contribution of the $(n+2)$, in total, compact dimensions, and from the eigenvalue of the $(3+n)$-dimensional spherical harmonic functions. An additional implicit dependence enters through the expression of the metric function $h(r)$. The latter is still given by Eq. (2), and it is thus characterized, as before, by two positive roots, r_H and r_C, and $(n+1)$ negative ones collectively denoted by r_m.

The above radial equation has been studied before, both analytically [11, 12] and numerically [14], in the absence of a bulk cosmological constant, to derive the spectrum of Hawking radiation from a higher-dimensional Schwarzschild-like black hole. Although the principles behind the emission of Hawking radiation in the bulk and on the brane are the same, the effect of the dimensionality of spacetime on the corresponding greybody factors and final emission rates was found to be different in the two "channels". In the presence of a bulk cosmological constant, we expect the existence of the second horizon r_C, to modify the low-energy bulk absorption coefficient in a way similar to the one for brane emission. Nevertheless, we anticipate the dimensionality of spacetime to have a much more explicit effect compared to the case of brane emission, where the number of additional dimensions appeared only implicitly in Eqs. (30) through the values of r_H and r_C. In the next two subsections, we focus on the emission of scalar fields in the bulk, and address the problem of finding the corresponding greybody factor both analytically and numerically.

4.1   Analytical results for scalar emission in the bulk

In this subsection, we follow the same methods as the ones presented in section 3.2 in order to derive analytically the low-energy absorption probability $|\mathcal{A}_{0,n}|^2$ and the high-energy absorption cross-section σ_g for the propagation of scalar fields in the background of the $(4+n)$-dimensional black hole given by Eqs. (1) and (2).

We will start by deriving the solution for the s-wave partial mode in the infrared limit, and compare it with the asymptotic solutions in the vicinity of the two horizons, r_H and r_C, expanded in the low-energy limit. For propagation in the bulk, the former can be derived by integrating the radial equation (41) in the intermediate radial regime $(r_H \ll r \ll r_C)$, for $\ell = 0$ and $\omega \to 0$. We then find

$$P(r) = C_1 \left[-\frac{\log r}{\mu} + \frac{\log(r - r_H)}{2k_H\,r_H^{2+n}} - \frac{\log(r_C - r)}{2k_C\,r_C^{2+n}} + \sum_{m=1}^{n+1} \frac{\log(r + r_m)}{2k_m\,r_m^{2+n}}\right] + C_2\,. \qquad (42)$$

In the above, k_i stands again for the surface gravity at the location of the ith root of the equation $h(r) = 0$, and it is still given by Eq. (19).
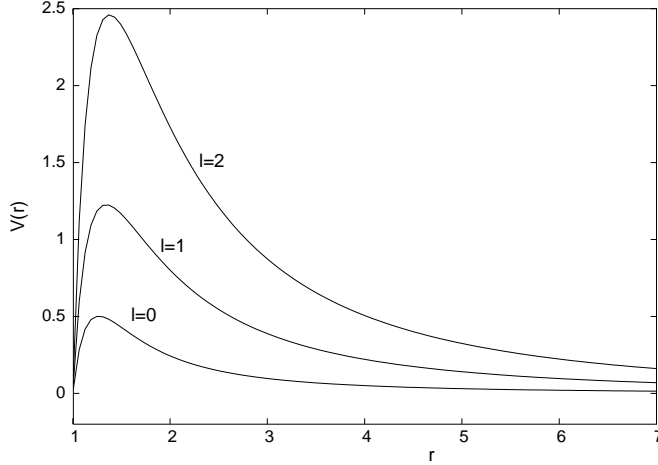
17

Figure 3: *The gravitational potential barrier $V(r)$ in the $(4+n)D$ SdS spacetime, for $n = 1$, $\mu = 1$, $\Lambda r_H^2 = 10^{-2}$ and $\ell = 0, 1$ and 2. The barrier vanishes again at $r_H = 1.0008$ and $r_C = 24.474$ but its height is significantly higher than on the brane.*

By using the definition $u(r) = r^{(n+2)/2} P(r)$, and the same tortoise coordinate defined in Eq. (20), the scalar field equation in the bulk (41) takes the Schrödinger-like form

$$-\frac{d^2 u}{dr_*^2} + h(r)\left[\frac{\ell(\ell + n + 1)}{r^2} + \frac{(n+2)\, h'(r)}{2r} + \frac{n(n+2)\, h(r)}{4r^2}\right] u = \omega^2 u\,, \qquad (43)$$

or, more explicitly,

$$-\frac{d^2 u}{dr_*^2} + h(r)\left[\frac{(2\ell + n + 1)^2 - 1}{4r^2} + \frac{\mu\,(n+2)^2}{4r^{n+3}} - \frac{\kappa_D^2 \Lambda\,(n+4)}{2\,(n+3)}\right] u = \omega^2 u\,. \qquad (44)$$

Once again, from the above expression, one may easily read the gravitational barrier $V(r)$ seen by a scalar field propagating in the higher-dimensional bulk. In Fig. 3, this gravitational barrier is shown for the indicative values of $n = 1$, $\mu = 1$, $\Lambda r_H^2 = 10^{-2}$ and $\ell = 0, 1$ and 2. As in the case of propagation on the brane, the barrier increases for increasing ℓ, therefore, it is the s-wave that is more likely to be emitted also in the bulk. Nevertheless, we notice that the height of the barrier is significantly higher compared to the one for propagation on the brane, therefore, we expect the emissivity of bulk scalar modes to be suppressed compared to the one of brane scalar modes, at least in the low- and intermediate-energy regime.

The metric function $h(r)$ is common for propagation both on the brane and in the bulk, therefore the potential vanishes at the same values of the radial coordinate, i.e. at r_H and r_C. In these asymptotic regimes, the solutions are given again by Eqs. (23)-(24), and their infrared limit by Eqs. (26) and (28). Comparing them with the s-wave solution (42), stretched towards the two horizons, will allow us to determine the relations between the set of coefficients A_1, (C_1, C_2) and (B_1, B_2). In particular, comparing $u^{(B)}(r_*)$, Eq. (26), with $r^{(n+2)/2} P(r)$, with the latter taken in the limit $r \to r_H$, we obtain the relations

$$C_1 = -i\omega\, r_H^{(n+2)/2} A_1\,, \qquad C_2 = \frac{A_1}{r_H^{(n+2)/2}} + \mathcal{O}(\omega)\,. \qquad (45)$$

18

Similarly, comparing $u^{(C)}(r_*)$, Eq. (28), with $r^{(n+2)/2} P(r)$, in the limit $r \to r_C$, we find in turn

$$C_1 = i\omega r_C^{(n+2)/2} \left(-B_1 + B_2 \right), \qquad C_2 = \frac{1}{r_C^{(n+2)/2}} \left(B_1 + B_2 \right) + \mathcal{O}(\omega). \qquad (46)$$

Rearranging the above set of constraints, we may easily derive the ratio B_2/B_1. Then, the reflection and absorption probabilities for the propagation of a scalar field in the bulk are found to be

$$|\mathcal{R}_{0,n}|^2 = \left| \frac{B_2}{B_1} \right|^2 = \left(\frac{r_C^{n+2} - r_H^{n+2}}{r_C^{n+2} + r_H^{n+2}} \right)^2, \qquad |\mathcal{A}_{0,n}|^2 = \frac{4 \left(r_C \, r_H \right)^{n+2}}{(r_C^{n+2} + r_H^{n+2})^2}. \qquad (47)$$

As in the case of brane emission, the absorption probability for emission in the bulk is not zero in the low-energy limit, contrary to what was derived for the propagation of a scalar field in the asymptotically-flat, $(4+n)$-dimensional background of a Schwarzschild black hole, where $|\mathcal{A}_{\ell,n}|^2 \sim (\omega r_H)^{2\ell+n+2}$ [11]. The above result differs also from the one derived in section 3.2 for brane propagation, Eq. (30), in that, as hinted at the beginning of section 4, the dimensionality of the spacetime in which the field propagates appears explicitly in the expression of the absorption probability at low energies. Table 3 shows the exact dependence of the absorption probability, for emission in the bulk at the low-energy limit, on the number of extra dimensions n and the bulk cosmological constant Λ, for $\mu = 1$. Similarly to the case of emission on the brane, the presence of a bulk cosmological constant enhances the absorption probability at low-energies and, thus, the emissivity of the black hole into the bulk, while a number of extra dimensions present, $n > 0$, have a suppressing effect on it. A simple comparison of the entries of Tables 1 and 3 confirms our expectation of a significantly reduced emission in the bulk of the dominant s-wave, compared to the one on the brane, for the same values of the free parameters of the theory.

Table 3: Absorption probabilities for emission in the bulk in the limit $\omega \to 0$

n	$|\mathcal{A}_{0,n}|^2$ (for $\Lambda r_H^2 = 10^{-2}$)	Λr_H^2	$|\mathcal{A}_{0,n}|^2$ (for $n = 1$)
0	1.417×10^{-2}	0	0
1	2.735×10^{-4}	10^{-4}	2.722×10^{-7}
2	4.006×10^{-6}	10^{-3}	8.611×10^{-6}
3	4.594×10^{-8}	10^{-2}	2.735×10^{-4}
5	3.445×10^{-12}	$10^{-1.5}$	1.554×10^{-3}
7	1.455×10^{-16}	10^{-1}	9.019×10^{-3}

We then turn to the high-energy regime, and to the geometrical optics limit value of the greybody factor. The equation describing the motion of a particle, with only one non-vanishing component of angular momentum, in a circular orbit around a black hole is given by Eq. (31), for propagation both in the bulk and on the brane – this equation is derived by fixing the values of all azimuthal angular coordinates θ_i to $\pi/2$, therefore the existence or not of n additional such variables does not change the final result. The

classically accessible regime is thus again given by $b < \min(r/\sqrt{h})$ with the minimum radial proximity given by Eq. (32). What nevertheless changes, in the case of propagation in a higher-dimensional black hole background, is the expression of the absorptive area of the black hole as a function of the critical radius b_c: as it was pointed out in Ref. [14], when carefully computed, this area comes out to be

$$A_p = \frac{2\pi}{(n+2)} \frac{\pi^{n/2}}{\Gamma[(n+2)/2]} \, b_c^{n+2} \,. \tag{48}$$

This area stands for the absorption cross-section, or greybody factor, at high energies. In the case of a higher-dimensional background with a bulk cosmological constant, that we study here, it takes the explicit form

$$\sigma_g = \frac{A_H}{\sqrt{\pi}\,(n+2)} \frac{\Gamma[(n+3)/2]}{\Gamma[(n+2)/2]} \times \tag{49}$$

$$\times \left\{ \left(\frac{n+1}{n+3}\right)\left(\frac{n+3}{2}\left[1 - \frac{2\kappa_D^2 \Lambda r_H^2}{(n+2)(n+3)}\right]\right)^{-2/(n+1)} - \frac{2\kappa_D^2 \Lambda r_H^2}{(n+2)(n+3)} \right\}^{-(n+2)/2},$$

upon making use of the expression for b_c given in Eq. (32). In the above, A_H is the horizon area of the $(4+n)$-dimensional SdS black hole given by

$$A_H = r_H^{n+2} A_{2+n} = r_H^{n+2}\,(2\pi)\,\pi^{(n+1)/2}\,\Gamma\left(\frac{n+3}{2}\right)^{-1}\,. \tag{50}$$

In Table 4, we give some indicative values of the greybody factor, in units of the area of the $(4+n)$-dimensional horizon A_H, for emission of scalar fields in the bulk at high-energies, for particular values of n and Λ, and for $\mu = 1$. Similarly to the case of emission on the brane, the presence of a bulk cosmological constant enhances the greybody factor, and increases the emissivity of the black hole into the bulk in the high-energy regime. In contrast to what happens in the emission of brane modes, however, choosing larger values for the number of transverse dimensions enhances the value of the greybody factor, instead of suppressing it. The same effect takes place also in the case of emission of scalar fields in the bulk by an asymptotically flat, higher-dimensional Schwarzschild black hole. The above formula (50) is a generalization of the one found in [14] for a non-vanishing bulk cosmological constant. Also in that simplified case, it may be shown that, for increasingly larger n, the greybody factor is indeed enhanced at high energies. This enhancement in the emission of highly-energetic scalar fields in the bulk, compared to the one on the brane, caused the boost in the bulk-to-brane emissivity for large values of n where the effect becomes significant [14].

Table 4: Greybody factors for emission in the bulk in the high-energy limit

n	(for $\Lambda r_H^2 = 10^{-2}$) $\sigma_g \ (A_H)$	Λr_H^2	(for $n = 0$) $\sigma_g \ (A_H)$	(for $n = 1$) $\sigma_g \ (A_H)$
0	1.7148	0	1.6875	1.6977
1	1.7105	10^{-4}	1.6878	1.6978
2	1.7757	10^{-3}	1.6902	1.6989
3	1.8535	10^{-2}	1.7148	1.7105
5	2.0117	$10^{-1.5}$	1.7778	1.7389
7	2.1622	10^{-1}	2.0241	1.8351

4.2 Numerical results for the greybody factor in the bulk

As in the case of brane emission, in order to derive accurate results for the emission of scalar fields in the bulk over the whole energy regime, we need to perform a numerical computation. The method followed here is identical to the one described in section 3.3. The numerical integration of the scalar bulk equation (41) starts from a point $r = r_H + \varepsilon$, close to the black hole horizon with the corresponding asymptotic solution satisfying the boundary conditions (33)-(34). The solution is then propagated towards the cosmological horizon and the numerical results are fitted by the appropriate asymptotic solution near r_C. As in the case of brane emission, a better fit is provided by making use of the alternative asymptotic solution (38) – although the scalar field equation and its general solution in the bulk is different from the ones on the brane, the asymptotic solution, for $r \to r_C$, has exactly the same form. The absorption probability $|\mathcal{A}_{\ell,n}|^2$ can then be defined by the ratio of the incoming fluxes at the black hole and cosmological horizon, and can easily follow once the amplitude of the *ingoing* wave B_1 is determined from the fit of our numerical results.

For emission in the bulk, the higher-dimensional formula, Eq. (12), for the absorption cross-section $\sigma_n(\omega)$ must be used. We are interested both in the effect of the cosmological constant and the dimensionality of spacetime on the behaviour of the greybody factor, and these effects are depicted in Figs. 4 (a,b). In Fig. 4a, we have kept the dimensionality of spacetime fixed, at $n = 1$, and varied the value of Λ. From the depicted curves, we may easily conclude that the absorption cross-section is enhanced as the value of Λ increases: as in the case of brane emission, the effect is more significant at the low-energy regime and less significant at the high-energy one, in complete accordance with the entries of Tables 3 and 4. For $\Lambda = 0$, we recover the well-known result of the greybody factor being equal to the horizon area of the higher-dimensional black hole [11, 14, 43]. Nevertheless, for non-vanishing values of Λ, the greybody factor diverges in the low-energy limit due to the fact that the absorption probability $|\mathcal{A}_{\ell,n}|^2$ acquires a non-vanishing constant value, in agreement to the analytical results of the previous subsection.
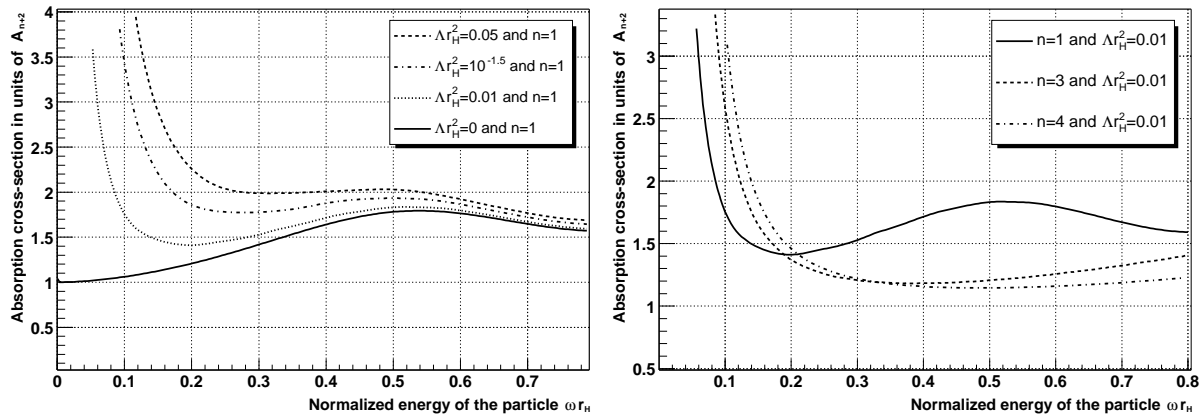
Figure 4: *The absorption cross-section $\sigma_n(\omega)$, for scalar emission in the bulk, versus the dimensionless parameter ωr_H:* (a) *the dimensionality of spacetime is fixed at $n = 1$, while Λr_H^2 takes the values $\{0, 10^{-2}, 10^{-1.5}, 0.05\}$ in Planck units;* (b) *the cosmological constant is fixed at $\Lambda r_H^2 = 10^{-2}$, and n takes the indicative values $\{1, 3, 4\}$.*

In Fig. 4b, on the other hand, we have kept the value of the cosmological constant fixed and varied the number of extra dimensions. The analytical results for the absorption probability $|\mathcal{A}_{0,n}|^2$, derived in the previous subsection, may have hinted towards the suppression of the greybody factor, too, in the low-energy regime. Nevertheless, not only is the suppression of $|\mathcal{A}_{0,n}|^2$, as a function of n, rather insignificant but also, as we may see from Eq. (12), there are actually two sources of enhancement of $\sigma_n(\omega)$, as n increases, in the low-energy regime: the multiplicative, n-dependent coefficient, and, more importantly, the factor $\omega^{-(n+2)}$. As a result, the greybody factor is indeed enhanced in the low-energy regime, as the curves in Fig. 4b also reveal. In the high-energy regime, finally, our curves seem to indicate that the greybody factor decreases with n, instead of increasing, as our analytical results showed. This is actually caused by the fact that, as in the case of emission in a flat spacetime [14], the high-energy limit behaviour of the greybody factor in the bulk is attained for fairly large values of ωr_H; as a result, the curves in Fig. 4b depict its behaviour only up to intermediate energy values, where $\sigma_n(\omega)$ is indeed suppressed with n. Extending our graph to higher values of energy leads to agreement with our analytical results.

5 Energy emission rates

In this section, we proceed to calculate the final energy emission rates for scalar fields by a higher-dimensional SdS black hole, both in the bulk and on the brane, by using the exact numerical results, derived in sections 3 and 4 for the corresponding absorption probabilities/greybody factors. Once this task is performed, we compare the amount of energy emitted in the "brane" and "bulk" channels, as a function of the cosmological

constant and the dimensionality of spacetime.

Before however writing down the formulae for the energy emission rates, we should first address the question of the consistent definition of the temperature of an SdS black hole. Equation (7), for the temperature of the black hole, was derived by making use of the definition of the surface gravity at the location of the black hole horizon, i.e.

$$k_H^2 = -\frac{1}{2} \lim_{r \to r_H} (D_M K_N) (D^M K^N) , \tag{51}$$

where

$$K = \gamma_t \frac{\partial}{\partial t} \tag{52}$$

is the timelike Killing vector, and γ_t a normalization constant. For a static and spherically-symmetric metric tensor, the above formula reduces to

$$k_H = \frac{1}{2} \frac{1}{\sqrt{-g_{tt}\, g_{rr}}} \left| g_{tt,r} \right|_{r=r_H} . \tag{53}$$

In fact, the above expression is derived provided the Killing vector is normalized according to the rule: $K_M K^M = -1$ [for the (-,+,...+) metric signature that we have used here] at the location where $|g_{tt}| = 1$. In the case of an asymptotically-flat Schwarzschild black hole, this happens at infinity where the spacetime reduces to a Minkowski flat one. However, in the presence of a cosmological constant, this asymptotically-flat regime does not exist. The normalization condition of the Killing vector can then be applied at the only point in the Schwarzschild-de-Sitter spacetime that shares the same characteristic with the infinity in the Schwarzschild spacetime, that is, no acceleration is necessary for an observer to stay there [44]. This point, for a higher-dimensional spacetime, is given in Eq. (6) and corresponds to the maximum value of the metric function $h(r)$. At the point $r = r_0$, the effect of the black hole attraction and the cosmological repulsion exactly cancel out. Once the proper normalization factor is included in the expression of the surface gravity, the correct expression for the temperature of the black hole comes out to be:

$$T_H = \frac{k_H}{2\pi} = \frac{1}{\sqrt{h(r_0)}} \frac{1}{4\pi r_H} \left[(n+1) - \frac{2\kappa_D^2 \Lambda}{(n+2)} r_H^2 \right] . \tag{54}$$

The above formula should then be used for the derivation of the decay radiation spectrum of a higher-dimensional SdS black hole, both in the bulk and on the brane. The corresponding expression, Eq. (11), takes the form

$$\frac{d^2 E(\omega)}{dt\, d\omega} = \sum_\ell N_{\ell,n} |\mathcal{A}_{\ell,n}|^2 \frac{\omega}{\exp\left(\omega/T_H\right) - 1} \frac{1}{2\pi} , \tag{55}$$

where $N_{\ell,n} = 2\ell + 1$, for brane emission, and

$$N_{\ell,n} = \frac{(2\ell + n + 1)\, (\ell + n)!}{\ell!\, (n+1)!} , \tag{56}$$
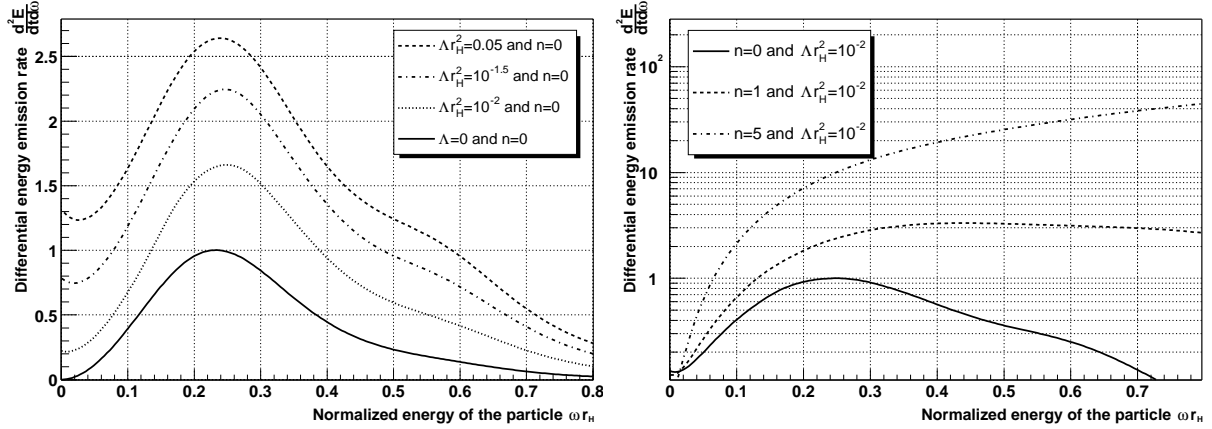
23

Figure 5: *The differential energy emission rate, for scalar emission on the brane, versus the dimensionless parameter ωr_H:* (a) *the dimensionality of spacetime is fixed at $n = 0$, while Λr_H^2 takes the values $\{0, 10^{-2}, 10^{-15}, 0.05\}$ in Planck units;* (b) *the cosmological constant is fixed at $\Lambda r_H^2 = 10^{-2}$, and n takes the indicative values $\{0, 1, 5\}$.*

for bulk emission, and the absorption probability takes the corresponding brane and bulk values. Figure 5 depicts the differential energy emission rates for emission on the brane, as a function of both Λ and n. In order to make the comparison easier, the maximum point of the lowest curve in both graphs, 5a and 5b, has been normalized to unity. In Fig. 5b, where Λ is fixed and n varies, the enhancement of the energy emission rate, by even orders of magnitude as n increases, is clear, and analogous to the behaviour found in the asymptotically-flat Schwarzschild spacetime [14]. A similar enhancement, but of a smaller scale, appears as the value of the cosmological constant increases. It is worth noting here that in the absence of the normalising factor $\sqrt{h(r_0)}$, an increase in the value of Λ leads to the decrease of the black hole temperature and thus to a suppression of the energy emission rate; however, the fact that the normalising factor is always smaller than unity gives a boost to T_H, that overcomes the decrease due to Λ.

A distinct feature of the decay spectrum of a SdS black hole is the non-vanishing value of the emission rate in the limit $\omega \to 0$. This is caused by the constant value of the absorption probability in the same limit, which as we saw leads to the divergence of the greybody factor at the low-energy regime but to a constant value of the energy emission rate. The larger the cosmological constant is, the larger the value of the absorption probability, and the larger the number of low-energy states that are emitted by the black hole. Whereas the total number of states that will be emitted by the black hole would come as a result of the combined effect of both Λ and n, the emission of a significantly number of extremely ultra-soft quanta on the brane would be a distinctive feature of the spectrum caused by the presence of a cosmological constant.

Figure 6 shows the energy emission rates for scalar fields in the bulk – the lowest curve in both graphs, 6a and 6b, has been again normalized to unity. As in the case of brane emission, the bulk energy emission rate is enhanced by the increase of both
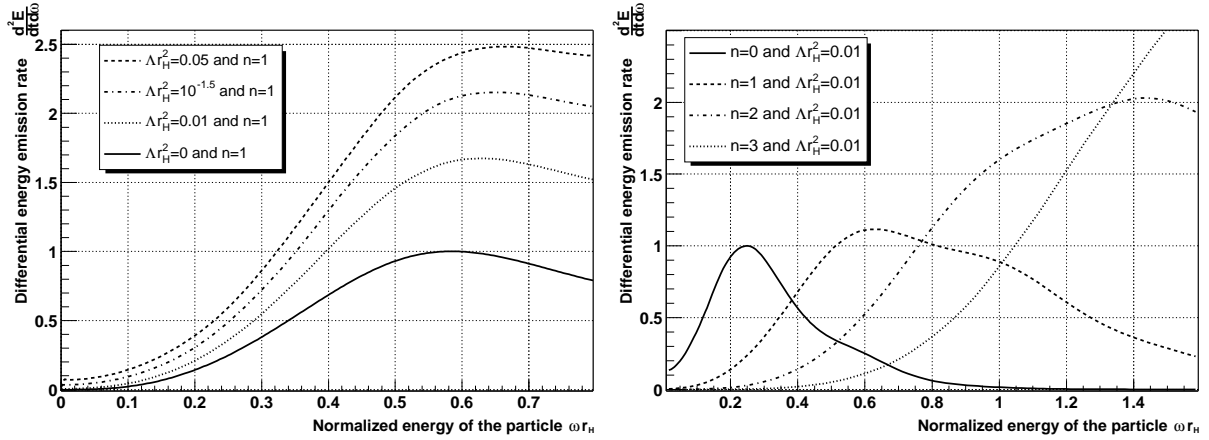
Figure 6: *The differential energy emission rate, for scalar emission in the bulk, versus the dimensionless parameter ωr_H:* (a) *the dimensionality of spacetime is fixed at $n = 1$, while Λr_H^2 takes the values $\{0, 10^{-2}, 10^{-1.5}, 0.05\}$ in Planck units;* (b) *the cosmological constant is fixed at $\Lambda r_H^2 = 10^{-2}$, and n takes the indicative values $\{0, 1, 2, 3\}$.*

the cosmological constant and the dimensionality of spacetime. We notice that, in both graphs, the peaks of all curves are shifted towards the right, i.e. to higher values of ωr_H, compared to the ones for brane emission. This is caused by the much smaller value of the absorption probability at the low-energy regime for emission in the bulk than on the brane. The total energy available for the emission of particles by the black hole is given, therefore any suppression in the emission of low-energy quanta leads to the emission of a larger number of high-energy ones.

Having derived the exact energy emission rates for emission both in the bulk and on the brane, we finally turn to the question of the bulk-to-brane relative emission rate. In the case of radiation emitted by a higher-dimensional Schwarzschild black hole, it was demonstrated [14] that most of the energy of the black hole goes into the "brane" channel, although the exact emissivity ratio was very much n-dependent. In the case of a SdS higher-dimensional black hole, we need to check the dependence of that ratio on both Λ and n; this dependence is shown in Figs. 7(a,b), respectively. Both figures reveal that this ratio is always smaller than unity, as in an asymptotically-flat spacetime. The presence of the cosmological constant – which can be seen as an addition to the energy of the emitted particle at every point $r = const.$ according to Eqs. (22) and (44) – becomes irrelevant at the high-energy regime, and the curves match those derived in the Schwarzschild case [14]. At the low-energy regime, though, and for fixed n – see Fig. 7a – the presence of the cosmological constant gives a boost to the bulk-to-brane ratio: this is due to the fact that a non-zero Λ lowers the height of the gravitational barrier for a bulk particle $(n + 4)(n + 2)/8$ times more than for a brane particle. On the other hand, increasing the number of extra dimensions leads to a strong suppression at the low-energy regime which, however, becomes milder as the energy increases causing the curves to start converge at around unity. This effect is obvious in Fig. 7b, and has its
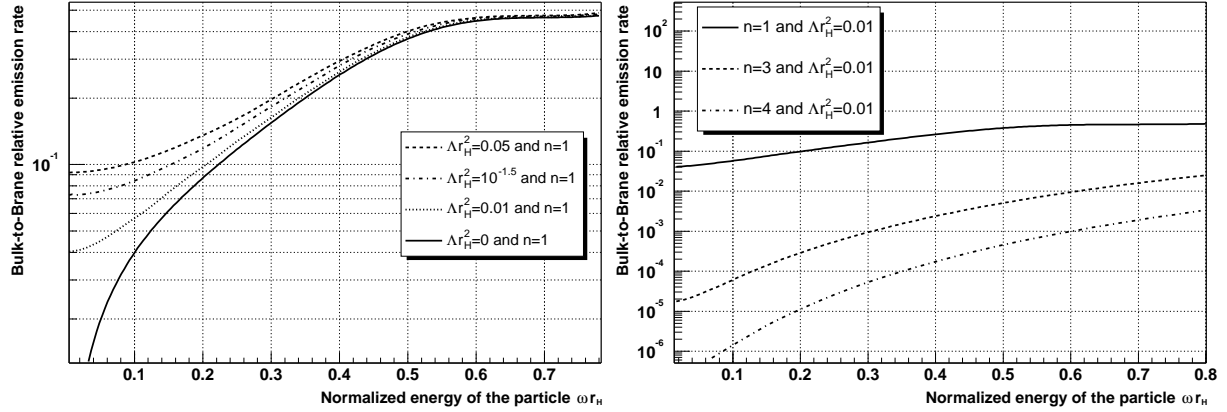
25

Figure 7: *The bulk-to-brane relative emission rate, for scalar emission, versus the dimensionless parameter ωr_H: (a) the dimensionality of spacetime is fixed at $n = 1$, while Λr_H^2 takes the values $\{0, 10^{-2}, 10^{-1.5}, 0.05\}$ in Planck units; (b) the cosmological constant is fixed at $\Lambda r_H^2 = 10^{-2}$, and n takes the indicative values $\{1, 3, 4\}$.*

source to the increased number of high-energy modes that are emitted in the bulk, an effect that becomes more significant for large values of n.

6   Conclusions

It has by now become clear that the spectrum of Hawking radiation, emitted by a black hole formed in a general geometrical background, can reveal valuable information for a variety of parameters that characterize this background. If the black hole is formed in a higher-dimensional spacetime, the shape and height of the characteristic energy emission curves can point towards a particular value of the number of spacelike dimensions that exist in nature [11, 13, 14]. In a similar way, the spectrum of Hawking radiation emanating from a black hole formed in the presence of the stringy-inspired Gauss-Bonnet term, is modified when the coupling parameter of this term varies [20]. Taking this idea further, in this work we have investigated how the radiation spectrum of a black hole formed in a D-dimensional de Sitter spacetime is affected by the presence of the positive cosmological constant.

In this paper, we have focused on the emission of Hawking radiation from a D-dimensional Schwarschild-de-Sitter (SdS) black hole emitted in the form of scalar fields - the emission of fields with non-zero spin is studied in a follow-up paper [45]. A higher-dimensional black hole can emit scalar fields both in the bulk and on the brane, therefore the study of the energy emission rates along both "channels" must be made. Scalar particles living on the brane are restricted to propagate on a slice of the higher-dimensional SdS spacetime, therefore, we had to derive first the induced gravitational background and then the corresponding equation of motion on the brane. An analytical calculation

26

led to the derivation of approximate formulae for the absorption coefficient and grey-body factor in the low- and high-energy regime, respectively. These results served also as guides for the numerical integration, that followed next and provided us with exact results for the greybody factor valid at all energy regimes. According to these results, the greybody factor for emission on the brane has a strong dependence on both the number of spacelike dimensions in nature and the curvature of spacetime: similarly to the case of an asymptotically-flat black hole, an increase in the value of n suppresses $\sigma_n(\omega)$; on the other hand, increasing the value of the cosmological constant enhances the same quantity, especially in the low-energy regime. By using similar analytical and numerical methods to study the emission of scalar fields in the bulk, we have found an equally strong dependence of the "bulk" greybody factor on n and Λ, although partially different: here, both the cosmological constant and a number of additional spacelike dimensions have a positive effect in the absorption cross-section.

Computing the final energy emission rates both on the brane and in the bulk was the following task. We had first to carefully redefine the temperature of the black hole in such a way as to take into account the non-asymptotic flatness of the SdS spacetime. This redefinition led to the introduction of an additional normalization factor whose presence proved to be crucial: in the absence of this factor, the temperature of the black hole increased with n but decreased with Λ; however, in its presence, both parameters caused an increase in the black hole temperature. Once the exact expressions of the black hole temperature and greybody factors were used, the energy emission rates in both "channels" were found to be strongly enhanced by the presence of either a number of additional dimensions or a cosmological constant. The rate of enhancement in the energy emission, in terms of the total number of dimensions and the value of the bulk cosmological constant, was not the same for the "brane" and "bulk" channel. The relative bulk-to-brane emission rate was then calculated in an attempt to estimate the amount of energy spent for emission in the bulk – the space transverse to the brane, and thus non-accessible to us – compared to the one spent on our brane. The bulk-to-brane ratio was found to be both n and Λ dependent, as expected, but it remained smaller than unity for all values of the two parameters considered. As a general rule, the emission of "brane" modes dominates in the low-energy regime but at the high-energy one, the "brane" and "bulk" rates become almost comparable.

Apart from the theoretical interest to study effects and processes in a curved space-time, motivated by the de Sitter and Anti-de Sitter / conformal field theory (CFT) cor-respondence, there is also a strong observational interest being fuelled by the prospect of the creation and decay of such small black holes in the near or far-future collider exper-iments able to probe the energy regime close to the fundamental gravitational scale M_*. Being able to obtain valuable information on the topological structure of our spacetime, including its dimensionality and curvature, from their Hawking radiation spectrum, might be a unique opportunity. According to our results, not only will the total number of par-ticles and energy emitted by these small black holes be a function of n and Λ, but each one of these parameters will leave a clear footprint in different energy regimes: while the cosmological constant becomes almost irrelevant at the high energy regime leaving the dimensionality of spacetime to determine the spectrum, it gives a unique feature at the

low-energy regime, through a Λ-dependent constant rate of emission of ultra-soft quanta. As scalar particles have proved to be rather elusive to detect, our present analysis will be extended, in a follow-up paper [45], to cover the emission of fermions and gauge fields, too – the data files used to construct the greybody factors and energy emission rates, for all species of fields and various values of n and Λ, can be found in a publicly accessible web-page [46].

As concluding remarks, let us comment on the validity and usefulness of the results derived here. The analysis performed in this work is general, and can be applied to any D-dimensional theory with either a low or high gravitational scale M_* – as long as the black hole mass remains much larger than this fundamental scale to ensure minimal back-reaction and absence of quantum effects. The number and size of additional dimensions also remained arbitrary, with the only assumption being made that the black hole horizon radius is much smaller than the smallest of the compact dimensions. An additional constraint relevant to the $(4+n)$-dimensional character of our analysis should be now re-instated: the frequency of the emitted particles must also be larger than $1/L$, otherwise they should be studied instead in the context of a purely 4-dimensional theory. This is in complete harmony with the results derived in this work: the effect of the number of extra dimensions is most obvious in the high-energy regime, where the emitted modes are clearly (4+n)-dimensional; in the low-energy regime, it is the effect of the cosmological constant that is the most important, an effect that remains a significant one even in the purely 4-dimensional case, as our results have shown. In the latter case, where no extra dimensions exist, and bulk and brane coincide, the production of small, classical black holes in colliders will be impossible, however, the energy emission rates derived here, and their dependence on the value of the cosmological constant, will still be of great use upon the detection of Hawking radiation emitted from small primordial black holes.

References

[1] N. Arkani-Hamed, S. Dimopoulos and G. R. Dvali, *Phys. Lett.* B **429**, 263 (1998) [hep-ph/9803315]; *Phys. Rev.* D **59**, 086004 (1999) [hep-ph/9807344]; I. Antoniadis, N. Arkani-Hamed, S. Dimopoulos and G. R. Dvali, *Phys. Lett.* B **436**, 257 (1998) [hep-ph/9804398].

[2] L. Randall and R. Sundrum, *Phys. Rev. Lett.* **83**, 3370 (1999) [hep-ph/9905221]; *Phys. Rev. Lett.* **83**, 4690 (1999) [hep-ph/9906064].

[3] K. Akama, *Lect. Notes Phys.* **176**, 267 (1982) [hep-th/0001113]; V. A. Rubakov and M. E. Shaposhnikov, *Phys. Lett.* B **125**, 139 (1983); *Phys. Lett.* B **125**, 136 (1983);

M. Visser, *Phys. Lett.* B **159**, 22 (1985) [hep-th/9910093];

G. W. Gibbons and D. L. Wiltshire, *Nucl. Phys.* **B287**, 717 (1987);

I. Antoniadis, *Phys. Lett.* B **246**, 377 (1990);

I. Antoniadis, K. Benakli and M. Quiros, *Phys. Lett.* B **331**, 313 (1994) [hep-ph/9403290];

J. D. Lykken, *Phys. Rev.* D **54**, 3693 (1996) [hep-th/9603133].

[4] T. Banks and W. Fischler, hep-th/9906038;

D. M. Eardley and S. B. Giddings, *Phys. Rev.* **D66**, 044011 (2002) [gr-qc/0201034];

H. Yoshino and Y. Nambu, *Phys. Rev.* **D66**, 065004 (2002) [gr-qc/0204060]; *Phys. Rev.* **D67**, 024009 (2003) [gr-qc/0209003];

E. Kohlprath and G. Veneziano, *JHEP* **0206**, 057 (2002) [gr-qc/0203093];

V. Cardoso, O. J. C. Dias and J. P. S. Lemos, *Phys. Rev.* D **67**, 064026 (2003)[hep-th/0212168];

E. Berti, M. Cavaglia and L. Gualtieri, *Phys. Rev.* **D69**, 124011 (2004) [hep-th/0309203];

V. S. Rychkov, *Phys. Rev.* D **70**, 044003 (2004) [hep-ph/0401116];

S. B. Giddings and V. S. Rychkov, *Phys. Rev.* D **70**, 104026 (2004) [hep-th/0409131];

O. I. Vasilenko, hep-th/0305067, hep-th/0407092.

[5] S. B. Giddings and S. Thomas, *Phys. Rev.* D **65**, 056010 (2002) [hep-ph/0106219];

S. Dimopoulos and G. Landsberg, *Phys. Rev. Lett.* **87**, 161602 (2001) [hep-ph/0106295];

S. Dimopoulos and R. Emparan, *Phys. Lett.* B **526**, 393 (2002) [hep-ph/0108060];

S. Hossenfelder, S. Hofmann, M. Bleicher and H. Stocker, *Phys. Rev.* **D66**, 101502 (2002) [hep-ph/0109085];

K. Cheung, *Phys. Rev. Lett.* **88**, 221602 (2002) [hep-ph/0110163];

R. Casadio and B. Harms, *Int. J. Mod. Phys.* **A17**, 4635 (2002) [hep-ph/0110255];

S. C. Park and H. S. Song, *J. Korean Phys. Soc.* **43**, 30 (2003) [hep-ph/0111069];

G. Landsberg, *Phys. Rev. Lett.* **88**, 181801 (2002) [hep-ph/0112061];

G. F. Giudice, R. Rattazzi and J. D. Wells, *Nucl. Phys.* B **630**, 293 (2002) [hep-ph/0112161];

E. J. Ahn, M. Cavaglia and A. V. Olinto, *Phys. Lett.* **B551**, 1 (2003)[hep-th/0201042];

T. G. Rizzo, *JHEP* **0202**, 011 (2002) [hep-ph/0201228]; hep-ph/0412087;

A. V. Kotwal and C. Hays, *Phys. Rev.* **D66**, 116005 (2002) [hep-ph/0206055];

A. Chamblin and G. C. Nayak, *Phys. Rev.* **D66**, 091901 (2002) [hep-ph/0206060];

T. Han, G. D. Kribs and B. McElrath, *Phys. Rev. Lett.* **90**, 031601 (2003) [hep-ph/0207003];

I. Mocioiu, Y. Nara and I. Sarcevic, *Phys. Lett.* **B557**, 87 (2003) [hep-ph/0310073];

M. Cavaglia, S. Das and R. Maartens, *Class. Quant. Grav.* **20**, L205 (2003) [hep-ph/0305223];

C. M. Harris, P. Richardson and B. R. Webber, *JHEP* **0308**, 033 (2003) [hep-ph/0307305];

D. Stojkovic, *Phys. Rev. Lett.* **94**, 011603 (2005) [hep-ph/0409124];

S. Hossenfelder, Mod. Phys. Lett. A **19**, 2727 (2004) [hep-ph/0410122];

C. M. Harris, M. J. Palmer, M. A. Parker, P. Richardson, A. Sabetfakhri and B. R. Webber, hep-ph/0411022.

[6] A. Goyal, A. Gupta and N. Mahajan, *Phys. Rev.* **D63**, 043003 (2001) [hep-ph/0005030];
J. L. Feng and A. D. Shapere, *Phys. Rev. Lett.* **88**, 021303 (2002) [hep-ph/0109106];
L. Anchordoqui and H. Goldberg, *Phys. Rev.* **D65**, 047502 (2002) [hep-ph/0109242];
R. Emparan, M. Masip and R. Rattazzi, *Phys. Rev.* **D65**, 064023 (2002) [hep-ph/0109287];
L. A. Anchordoqui, J. L. Feng, H. Goldberg and A. D. Shapere, *Phys. Rev.* D **65**, 124027 (2002) [hep-ph/0112247]; *Phys. Rev.* **D68**, 104025 (2003) [hep-ph/0307228];
Y. Uehara, *Prog. Theor. Phys.* **107**, 621 (2002) [hep-ph/0110382];
J. Alvarez-Muniz, J. L. Feng, F. Halzen, T. Han and D. Hooper, *Phys. Rev.* D **65**, 124015 (2002) [hep-ph/0202081];
A. Ringwald and H. Tu, *Phys. Lett.* B **525**, 135 (2002) [hep-ph/0111042];
M. Kowalski, A. Ringwald and H. Tu, *Phys. Lett.* B **529**, 1 (2002) [hep-ph/0111042];
E. J. Ahn, M. Ave, M. Cavaglia and A. V. Olinto, *Phys. Rev.* D **68**, 043004 (2003) [hep-ph/0306008];
E. J. Ahn, M. Cavaglia and A. V. Olinto, *Astropart. Phys.* **22**, 377 (2005) [hep-ph/0312249];
A. Cafarella, C. Coriano and T. N. Tomaras, hep-ph/0410358.

[7] P. Kanti, *Int. J. Mod. Phys.* A **19**, 4899 (2004) [hep-ph/0402168].

[8] M. Cavaglia, *Int. J. Mod. Phys.* **A18**, 1843 (2003) [hep-ph/0210296];
G. Landsberg, *Eur. Phys. J.* **C33**, S927 (2004) [hep-ex/0310034];
K. Cheung, hep-ph/0409028;
S. Hossenfelder, hep-ph/0412265.

[9] R. C. Myers and M. J. Perry, *Annals Phys.* **172**, 304 (1986).

[10] P. C. Argyres, S. Dimopoulos and J. March-Russell, *Phys. Lett.* B **441**, 96 (1998) [hep-th/9808138].

[11] P. Kanti and J. March-Russell, *Phys. Rev.* D **66**, 024023 (2002) [hep-ph/0203223].

[12] V. P. Frolov and D. Stojkovic, *Phys. Rev.* D **66**, 084002 (2002) [hep-th/0206046].

[13] P. Kanti and J. March-Russell, *Phys. Rev.* D **67**, 104019 (2003) [hep-ph/0212199].

[14] C. M. Harris and P. Kanti, *JHEP* **0310**, 014 (2003) [hep-ph/0309054].

[15] V. P. Frolov and D. Stojkovic, *Phys. Rev.* D **67**, 084004 (2003) [gr-qc/0211055].

[16] D. Ida, K. y. Oda and S. C. Park, *Phys. Rev.* D **67**, 064025 (2003), *Erratum-ibid.* D **69**, 049901 (2004)[hep-th/0212108].

[17] W. T. Zaumen, *Nature* **247**, 530 (1974);
B. Carter, *Phys. Rev. Lett.* **33**, 558 (1974);
A. A. Starobinskii and S. M. Churilov, *Sov. Phys.-JETP* **38**, 1 (1974);
G. W. Gibbons, *Commun. Math. Phys.* **44**, 245 (1975);
W. G. Unruh, *Phys. Rev.* D **14**, 3251 (1976).

[18] D. N. Page, *Phys. Rev.* **D13**, 198 (1976); *Phys. Rev.* **D14**, 1509 (1976); *Phys. Rev.* **D14**, 3260 (1976); *Phys. Rev.* **D16**, 2402 (1977).

[19] N. Sanchez, *Phys. Rev.* **D16**, 937 (1977); *Phys. Rev.* **D18**, 1030 (1978); *Phys. Rev.* **D18**, 1798 (1978).

[20] A. Barrau, J. Grain and S. O. Alexeyev, *Phys. Lett.* **B584**, 114 (2004).

[21] S. Perlmutter *et al.* [Supernova Cosmology Project Collaboration], *Astrophys. J.* **517**, 565 (1999) [astro-ph/9812133];
A. G. Riess *et al.* [Supernova Search Team Collaboration], *Astrophys. J.* **607**, 665 (2004) [astro-ph/0402512].

[22] R. L. Mallett, *Phys. Rev.* D **33**, 2201 (1986).

[23] P. C. W. Davies, L. H. Ford and D. N. Page, *Phys. Rev.* D **34**, 1700 (1986).

[24] W. H. Huang, Class. Quant. Grav. **9**, 1199 (1992) [hep-th/0408166].

[25] R. Bousso and S. W. Hawking, *Phys. Rev.* D **57**, 2436 (1998) [hep-th/9709224].

[26] O. J. C. Dias and J. P. S. Lemos, hep-th/0410279.

[27] A. J. M. Medved, *Phys. Rev.* D **66**, 124009 (2002) [hep-th/0207247].

[28] H. Kodama and A. Ishibashi, *Prog. Theor. Phys.* **110**, 901 (2003) [hep-th/0305185];
Prog. Theor. Phys. **111**, 29 (2004) [hep-th/0308128].

[29] H. Maeda, T. Torii and T. Harada, gr-qc/0501042.

[30] C. Molina, *Phys. Rev.* D **68**, 064007 (2003) [gr-qc/0304053];
R. A. Konoplya, *Phys. Rev.* D **68**, 124017 (2003) [hep-th/0309030];
V. Cardoso, O. J. C. Dias and J. P. S. Lemos, *Phys. Rev.* D **70**, 024002 (2004) [hep-th/0401192];
L. Vanzo and S. Zerbini, *Phys. Rev.* D **70**, 044030 (2004) [hep-th/0402103];
D. P. Du, B. Wang and R. K. Su, *Phys. Rev.* D **70**, 064024 (2004) [hep-th/0404047];
J. Natario and R. Schiappa, hep-th/0411267.

[31] F. Mellor and I. Moss, *Phys. Rev.* D **41**, 403 (1990);
P. R. Brady, C. M. Chambers, W. G. Laarakkers and E. Poisson, *Phys. Rev.* D **60**, 064003 (1999) [gr-qc/9902010];
B. Wang, E. Abdalla and R. B. Mann, *Phys. Rev.* D **65**, 084006 (2002) [hep-th/0107243];

V. Suneeta, *Phys. Rev.* D **68**, 024020 (2003) [gr-qc/0303114];

J. x. Tian, Y. x. Gui, G. h. Guo, Y. Lv, S. h. Zhang and W. Wang, *Gen. Rel. Grav.* **35**, 1473 (2003) [gr-qc/0304009];

A. Zhidenko, *Class. Quant. Grav.* **21**, 273 (2004) [gr-qc/0307012];

C. Molina, D. Giugno, E. Abdalla and A. Saa, *Phys. Rev.* D **69**, 104013 (2004) [gr-qc/0309079];

T. R. Choudhury and T. Padmanabhan, *Phys. Rev.* D **69**, 064033 (2004) [gr-qc/0311064];

R. A. Konoplya and A. Zhidenko, *JHEP* **0406**, 037 (2004) [hep-th/0402080];

V. Cardoso, J. Natario and R. Schiappa, hep-th/0403132;

A. A. Smirnov, gr-qc/0412073.

[32] F.R. Tangherlini, *Nuovo. Cim.* **27**, 636 (1963).

[33] S. W. Hawking, *Commun. Math. Phys.* **43**, 199 (1975).

[34] S. S. Gubser, I. R. Klebanov and A. A. Tseytlin, *Nucl. Phys.* **B499**, 217 (1997).

[35] E. Newman and R. Penrose, *J. Math. Phys.* **3**, 566 (1962).

[36] S. Chandrasekhar, *The Mathematical Theory of Black Holes* (Oxford University Press, New York, 1983).

[37] J. N. Goldberg, A. J. MacFarlane, E. T. Newman, F. Rohrlich and E. C. Sudarshan, *J. Math. Phys.* **8**, 2155 (1967).

[38] Y. Gürcel, V. D. Sandberg, I. D. Novikov and A. A. Starobinsky, *Phys. Rev.* D **19**, 413 (1979); *Phys. Rev.* D **20**, 1260 (1979).

[39] P. R. Brady, C. M. Chambers, W. Krivan and P. Laguna, *Phys. Rev.* D **55**, 7538 (1997) [gr-qc/9611056].

[40] C. W. Misner, K. T. Thorne and J. A. Wheeler, *Gravitation* (Freeman, San Fransisco, 1973).

[41] R. Emparan, G. T. Horowitz and R. C. Myers, *Phys. Rev. Lett.* **85**, 499 (2000) [hep-th/0003118].

[42] C. Muller, in *Lecture Notes in Mathematics: Spherical Harmonics* (Springer-Verlag, Berlin-Heidelberg, 1966).

[43] E. l. Jung, S. H. Kim and D. K. Park, *Phys. Lett.* **B586**, 390 (2004) [hep-th/0311036]; *JHEP* **0409**, 005 (2004) [hep-th/0406117]; *Phys. Lett.* B **602**, 105 (2004) [hep-th/0409145]; E. Jung and D. K. Park, *Class. Quant. Grav.* **21**, 3717 (2004) [hep-th/0403251].

[44] R. Bousso and S. W. Hawking, *Phys. Rev.* D **54**, 6312 (1996) [gr-qc/9606052].

[45] J. Grain, P. Kanti and A. Barrau, in progress.

[46] http://lpsc.in2p3.fr/ams/greybody/ .